Journal of Inflammation Research

Dovepress
open access to scientific and medical research

Open Access Full Text Article

ORIGINAL RESEARCH

Differential Regional Vulnerability of the Brain to Mild Neuroinflammation Induced by Systemic LPS Treatment in Mice

Hyeji Jung[1], Hyojeong Lee[1], Dongwook Kim[1], Eunji Cheong[2], Young-Min Hyun[3], Je-Wook Yu[4], Ji Won Um[1]

[1]Department of Brain Sciences, Daegu Gyeongbuk Institute of Science and Technology (DGIST), Daegu, 42988, Korea; [2]Department of Biotechnology, College of Life Science and Biotechnology, Yonsei University, Seoul, 03722, Korea; [3]Department of Anatomy and Brain Korea 21 PLUS Project for Medical Science, Yonsei University College of Medicine, Seoul, 03722, Korea; [4]Department of Microbiology and Immunology, Institute for Immunology and Immunological Diseases, Brain Korea 21 PLUS Project for Medical Science, Yonsei University College of Medicine, Seoul, 03722, Korea

Correspondence: Ji Won Um, Email jiwonum@dgist.ac.kr

Background: Peripheral inflammation-triggered mild neuroinflammation impacts the brain and behavior through microglial activation. In this study, we performed an unbiased analysis of the vulnerability of different brain areas to neuroinflammation induced by systemic inflammation.

Methods: We injected mice with a single low dose of LPS to induce mild inflammation and then analyzed microglial activation in 34 brain regions by immunohistochemical methods and whole-brain imaging using multi-slide scanning microscopy. We also conducted quantitative RT-PCR to measure the levels of inflammatory cytokines in selected brain regions of interest.

Results: We found that microglia in different brain regions are differentially activated by mild, LPS-induced inflammation relative to the increase in microglia numbers or increased CD68 expression. The increased number of microglia induced by mild inflammation was not attributable to infiltration of peripheral immune cells. In addition, microglia residing in brain regions, in which a single low-dose injection of LPS produced microglial changes, preferentially generated pro-inflammatory cytokines.

Conclusion: Our results suggest that mild neuroinflammation induces regionally different microglia activation, producing pro-inflammatory cytokines. Our observations provide insight into induction of possible region-specific neuroinflammation-associated brain pathologies through microglial activation.

Keywords: neuroinflammation, microglia, inflammatory cytokines, lipopolysaccharide, regional vulnerability

Background

Neuroinflammation reflects the complex interplay between acute and chronic responses of cells within the central nervous system (CNS).[1] Neuroinflammation results in synapse loss and contributes to the initiation and progression of neurodegenerative diseases, including Alzheimer's disease (AD), and Parkinson's disease, as well as neuropsychiatric disorders, such as schizophrenia and depression.[2] Pathological events that evoke systemic inflammation induce neuroinflammation and subsequently impair cognition.[3] Under such pathological conditions, peripheral immune cells, which release various inflammatory cytokines, can readily infiltrate into the brain through the loss of blood-brain barrier integrity.[4,5] Peripheral inflammation is also sensed through the vagal nerve or gut-to-brain axis to alert the CNS against the threats,[6,7] even though the mechanisms by which systemic inflammation elicits afferent nervous signals in the CNS are not clearly understood.

Systematic inflammation can be experimentally induced by peripheral injection of lipopolysaccharide (LPS), a potent endotoxin released from gram-negative bacteria that binds to Toll-like receptor-4. LPS administration activates the innate immune system and induces microglial activation to produce neuroinflammatory responses in the brain. Thus, mice with acutely administered LPS are a widely used animal model for investigating the relationship between neuroinflammation

Received: 10 February 2022
Accepted: 16 May 2022
Published: 23 May 2022

and cognition. Despite the abundant literature on the subject, different observations have been reported regarding the presence of the major pro-inflammatory cytokines in the brain after LPS administration. These discrepancies could be attributable to numerous differences in experimental detail from one study to the next, including the mouse strain used, purity of LPS administered, administration route (eg, intraperitoneal injection (i.p.) vs intracerebroventricular injection), quantity of LPS administered, and duration of administration (acute vs chronic)—all of which may influence the outcome. LPS exposure causes sustained microglial activation in different brain areas, notably including the hippocampus, anterior cingulate cortex (ACC), cerebellum, amygdala and substantia nigra (SN).[8–12] Microglial activation induced by systemic inflammation is often associated with molecular and cellular changes, such as neuronal cell loss, synaptic deficits, altered levels of neurotransmitters and oxidative stress. Neuroinflammation is also accompanied by behavioral changes related to specific brain regions. For example, LPS administration in young mice induces microglial activation in the ACC resulting in a subsequent increase in the development of depressive symptoms.[8]

Despite intensive investigation, it has remained unclear which brain regions are vulnerable to neuroinflammation in response to systemic inflammation. In this study, we administered mice with a single low dose of LPS to induce mild inflammation in the periphery and then analyzed different brain regions to identify regional dependency that may be targets for the effects of low-grade inflammation.

Materials and Methods

Animals

All C57BL/6N and CCR2$^{RFP/+}$ mice (Jackson Laboratory; #017586) were maintained and handled in accordance with protocols (DGIST-IACUC-20122401-0004) approved by the Institutional Animal Care and Use Committee (IACUC) of the Daegu Gyeongbuk Institute of Science and Technology (DGIST). Mice were maintained on a 12:12-h light: dark cycle under standard, temperature (22–26 °C)- and humidity (40–60%)-controlled laboratory conditions, and received water and food *ad libitum*. Mice were group-housed at up to four animals per cage. All experimental procedures were performed on 44 mice and were conducted according to the guidelines and protocols for rodent experimentation approved by the IACUC of DGIST. Only male mice were analyzed in the current study to avoid the biological variability arising from sex differences.

Antibodies

The following commercially available antibodies were used: rabbit polyclonal anti-Iba-1 (Fujifilm Wako, Cat# 016–20001; RRID: AB_839506) and rat monoclonal anti-CD68 (clone FA-11; Bio-Rad, Cat# MCA1957GA; RRID: AB_324217).

LPS Injection and Immunohistochemistry

Eight-week-old mice were subjected to 1 or 2 daily intraperitoneal injections of saline or 0.5 mg/kg LPS (from *Escherichia coli* O111:B4, L3012, Sigma, Lot# 12170308). LPS was first dissolved in distilled water, diluted to a final concentration of 0.05 mg/mL with PBS, and injected into mice in a volume of 10 μL per 1 gram of mouse body weight. For the two daily doses, the LPS solution was injected twice at a 24-h-interval. Twenty-four hours after the final injection, mice were deeply anaesthetized by inhalation of isoflurane and immediately perfused, first with phosphate-buffered saline (PBS) for 3 min and then with 4% paraformaldehyde for 5 min. Brains were dissected out, fixed in 4% paraformaldehyde overnight, then incubated with 30% sucrose (in PBS) overnight and sliced into 40-μm-thick coronal sections using a cryotome (Model CM-3050-S; Leica Biosystems). A total of 34 brain regions associated with neuropsychiatric disorders were selected and subjected to IHC analyses. Sections were permeabilized by incubating with 0.2% Triton X-100 in PBS containing 5% bovine serum albumin and 5% horse serum for 1 h. For immunostaining, brain sections (3 slices/mouse) were incubated for 16 h at 4 °C with primary antibodies against Iba-1 and CD68, diluted 1:400 and 1:300, respectively, in the same blocking solution. Sections were washed three times in PBS and incubated with appropriate Cy3- or FITC-conjugated secondary antibodies (Jackson ImmunoResearch) for 2 h at room temperature. After three washes with PBS, sections were mounted onto glass slides (Superfrost Plus; Fisher Scientific) with

Vectashield mounting medium (H-1200; Vector Laboratories). Whole selected brain sections were scanned using a confocal microscope (LSM800; Carl Zeiss) or a slide scanner (Axio Scan.Z1; Carl Zeiss) with a 20 × objective lens; all image settings were kept constant during image acquisition. Z-stack images obtained with the slide scanner were converted to maximal projections, and the acquired images were further processed using ZEN software installed in Axio Scan.Z1. Boundaries of each anatomical subregions in five brain sections (Bregma level 1.98, 0.98, −1.82, −3.16, and −4.6) were manually defined according to Paxinos and Franklin's, The Mouse Brain in Stereotaxic Coordinates (4th edition). After clearly distinguishing each anatomical subregion during alignment, the density of Iba-1$^+$ immunoreactive cells in each brain region was analyzed in a blinded manner using MetaMorph software (Molecular Devices Corp.).

Quantitative Real-Time Polymerase Chain Reaction

Cortex, hippocampus, habenula (Hb), and ventral tegmental area (VTA) were rapidly dissected or punched out from 2 to 4 slices of acute brain sections (200-μm thick) with reference to the Mouse Brain Atlas, and prepared using a vibratome (Leica, VT1000S). Harvested brain tissues were incubated with 1 mL of TRIzol reagent (Invitrogen) at room temperature for 5 min. After phenol-chloroform extraction, RNA in the upper aqueous phase was isolated and precipitated using 2-propanol. Precipitated RNA pellets were washed twice with 75% Ethanol in DEPC-treated water and dissolved in DEPC water. cDNA (Hb/VTA, 120 ng; hippocampus/cortex, 500 ng) was synthesized from RNA by reverse transcription using a ReverTra Ace-α kit (Toyobo). Quantitative polymerase chain reaction (qPCR) was performed on a CFX96 Touch Real-Time PCR system (BioRad) using TB Green premix (Takara). After the initial denaturation (95°C, 15 min), 45 cycles of a two-step thermocycles consist of denaturation (94°C, 15 s) and annealing/extension (61°C, 40 s) were carried out. All reactions were performed in duplicates and the ubiquitously expressed *Gapdh* gene was used to normalize the expression levels of cytokines in each sample. The following target genes were amplified using the indicated primer pairs: mouse *IL-1β*, 5'-GGT GTG TGA CGT TCC CAT TA-3' (forward) and 5'-ATT GAG GTG GAG AGC TTT CAG-3' (reverse); mouse *TNFα*, 5'-TTG TCT ACT CCC AGG TTC TCT-3' (forward) and 5'-GAG GTT GAC TTT CTC CTG GTA TG-3' (reverse); mouse *TGF-β1*, 5'-CTG AAC CAA GGA GAC GGA ATA C-3' (forward) and 5'-GGG CTG ATC CCG TTG ATT T-3' (reverse); mouse *IL-4*, 5'-GAA GAA CAC CAC AGA GAG TGA G-3' (forward) and 5'-TGC AGC TCC ATG AGA ACA C −3' (reverse); and rat/mouse *Gapdh*, 5'-ACA TGG TCT ACA TGT TCC AG-3' (forward) and 5'-TCG CTC CTG GAA GAT GGT GAT-3' (reverse).

Statistical Analysis

All the data are presented as means ± standard error of the mean (SEM). The data were statistically evaluated using a Mann–Whitney *U*-test. Prism 8.0 (GraphPad Software) was used for analysis of data and preparation of bar graphs. *P*-values <0.05 were considered to be statistically significant.

Results

Microglial Activation Occurs in a Brain Region-Dependent Manner in Response to Mild, LPS-Induced Inflammation

To determine which brain regions are vulnerable to LPS-induced systemic inflammation, we injected mice with LPS once a day for 1 or 2 d, and then 24 h after LPS injection assessed microglia activation in various brain regions by immunohistochemical analyses using antibodies against Iba-1 (ionized calcium-binding adapter molecule-1), a specific biomarker for microglial cells. We chose 34 brain areas that have been associated with various neuropsychiatric disorders for anatomical analyses.[13–16] Using AxioScanner, we examined the number of Iba-1+ cells in 34 brain regions using the same imaging conditions (Table 1, Figure 1, Figures S1 and S2). We found that the number of microglia was drastically increased in all examined brain regions of mice injected with LPS twice on two consecutive days. Interestingly, a single i.p. injection of LPS induced an increase in the number of Iba-1+ microglia in specific brain regions, namely the medial habenula (MHb), lateral habenula (LHb), medial septum (MS), nucleus accumbens (NAc), claustrum (Cla), infralimbic cortex (ILC), piriform cortex (PC), retrosplenial cortex (RSC), auditory cortex (AC), and entorhinal cortex (EC). Among

Table 1 Summary of Microglia Numbers in Various Brain Areas

Region	A Single Dose					Two Daily Doses				
	Means ± SEMs		Fold Change	Statistics	p value	Means ± SEMs		Fold Change	Statistics	p value
	PBS	LPS				PBS	LPS			
ACC	186.68 ± 13.52	203.01 ± 10.43	1.09	ns	0.3453	183.44 ± 10.84	265.89 ± 9.98	1.45	****	<0.0001
PLC	198.49 ± 14.97	230.83 ± 11.55	1.16	ns	0.1160	200.69 ± 9.13	308.46 ± 7.95	1.54	****	<0.0001
ILC	211.47 ± 15.58	248.56 ± 11.96	1.18	*	0.0295	183.37 ± 10.39	319.63 ± 8.47	1.74	****	<0.0001
Cla	239.62 ± 15.66	285.02 ± 12.91	1.19	*	0.0209	254.64 ± 15.14	373.86 ± 5.95	1.47	****	<0.0001
IC	235.15 ± 14.63	263.80 ± 10.2	1.12	ns	0.0675	231.41 ± 13.86	344.46 ± 10.46	1.49	****	<0.0001
LS	134.04 ± 15.82	127.25 ± 19.09	0.95	ns	0.7130	170.31 ± 7.08	252.37 ± 8.61	1.48	****	<0.0001
MS	105.26 ± 16.16	166.53 ± 12.62	1.58	**	0.0057	88.91 ± 5.86	233.42 ± 11.13	2.63	****	<0.0001
MC	208.38 ± 16.29	214.54 ± 9.36	1.03	ns	0.3892	207.34 ± 12.29	312.2 ± 9.51	1.51	****	<0.0001
NAcc	259.46 ± 19.35	311.32 ± 12.38	1.20	*	0.0209	241.62 ± 15.07	392.6 ± 6.09	1.62	****	<0.0001
NAcsh	206.01 ± 14.99	256.27 ± 9.25	1.24	**	0.0049	175.2 ± 9.68	316.01 ± 7.8	1.80	****	<0.0001
SC	165.55 ± 14.33	182.87 ± 11.29	1.10	ns	0.2496	197.49 ± 12.94	307.25 ± 11.52	1.56	****	<0.0001
PC	221.32 ± 18.05	281.13 ± 10.33	1.27	**	0.0020	199.69 ± 15.51	342.42 ± 8.06	1.71	****	<0.0001
RSC	180.04 ± 9.57	232.29 ± 12.75	1.29	**	0.0043	160.45 ± 7.5	272.92 ± 15.73	1.70	****	<0.0001
dCA1	232.88 ± 12.65	221.32 ± 19.55	0.95	ns	0.4864	217.83 ± 8.29	295.49 ± 8.18	1.36	****	<0.0001
dCA3	127.19 ± 18.11	158 ± 19.8	1.24	ns	0.3046	182.41 ± 14.15	329.71 ± 31.14	1.81	****	<0.0001
dDG	167.31 ± 17.04	201.41 ± 19.99	1.20	ns	0.2671	227.26 ± 16.35	337.84 ± 13.37	1.49	****	<0.0001
LHb	85.7 ± 17.88	138.85 ± 19.32	1.62	*	0.0145	81.47 ± 16.7	228.47 ± 17.48	2.80	****	<0.0001
MHb	67.52 ± 12.11	176.5 ± 20.55	2.61	***	0.0003	138.1 ± 23.69	340.47 ± 17.8	2.47	****	<0.0001
PVT	45.41 ± 9.86	74.5 ± 16.01	1.64	ns	0.1261	85.12 ± 15.31	245.38 ± 18.58	2.88	****	<0.0001
MDT	36.46 ± 8.03	43.81 ±8.99	1.20	ns	0.5949	85.49 ± 17.2	283.24 ± 29.54	3.31	****	<0.0001
CM	46.63 ± 10.39	53.19 ± 10.45	1.14	ns	0.4363	92.58 ± 18.38	284.06 ± 30.48	3.07	****	<0.0001
CeA	280.6 ± 12.46	257.89 ± 20.93	0.92	ns	0.7130	167.07 ± 5.76	332.29 ± 21.36	1.99	****	<0.0001

BLA	334.98 ± 13.68	305.71 ± 18.56	0.91	ns	0.7130	238.93 ± 8.56	345.37 ± 12.33	1.45	****	<0.0001
DMH	203.69 ± 13.41	227.69 ± 18.89	1.12	ns	0.2854	134.26 ± 10.39	260.37 ± 9.96	1.94	****	<0.0001
VMH	228.17 ± 19.21	251.15 ± 15.1	1.10	ns	0.3314	142.52 ± 13.99	351.25 ± 25.18	2.46	****	<0.0001
AC	152.84 ± 13.57	193.54 ± 13.48	1.27	*	0.0453	149.79 ± 7.02	240.7 ± 9.65	1.61	****	<0.0001
EC	192.74 ± 13.99	275.04 ± 11.56	1.43	***	0.0001	134.23 ± 8.49	267.88 ± 10.95	2.00	****	<0.0001
vCA1	154.84 ± 6.72	173.31 ± 11.26	1.12	ns	0.1873	95.82 ± 5.65	221.24 ± 6.24	2.31	****	<0.0001
vCA3	142.44 ± 8.99	152 ± 15.16	1.07	ns	0.8702	99.78 ± 4	211.93 ± 6.22	2.12	****	<0.0001
vDG	142.05 ± 13.14	153.93 ± 17.68	1.08	ns	0.9674	141.94 ± 6.45	257.73 ± 6.93	1.82	****	<0.0001
SN	118.34 ± 12.29	154.9 ± 17.94	1.31	ns	0.2017	73.55 ± 6.13	324.05 ± 10.89	4.41	****	<0.0001
VTA	50.59 ± 5.62	55.59 ± 8.69	1.10	ns	0.9349	20.56 ± 2.35	179.62 ± 12.14	8.73	****	<0.0001
PAG	223.49 ± 13.38	146.19 ± 22.52	0.65	*	0.0128	161.79 ± 11.7	283.67 ± 8.3	1.75	****	<0.0001
DRN	155.29 ± 23.58	94.14 ± 10.96	0.61	*	0.0453	139.03 ± 18.02	265.57 ± 7.81	1.91	****	<0.0001

Notes: Quantification of the density (mm^{-2}) of iba-1^{+} cells. Data are means ± SEMs (n = 14~15 sections from 5 mice; *$p < 0.05$, ** $p < 0.01$, ***$p < 0.001$, ****$p < 0.0001$, ns, not significant; Mann–Whitney *U*-test).

Abbreviations: ACC, anterior cingulate cortex; PLC, prelimbic cortex; ILC, infralimbic cortex; Cla, claustrum; IC, insular cortex; LS, lateral septum; MS, medial septum; MC, motor cortex; NAcc, nucleus accumbens core; NAcsh, nucleus accumbens shell; SC, somatosensory cortex; PC, piriform cortex; RSC, retrosplenial cortex; dCA1, dorsal cornu ammonis 1; dCA3, dorsal cornu ammonis 3; dDG, dorsal dentate gyrus; LHb, lateral habenula; MHb, medial habenula; PVT, paraventricular thalamic nucleus; MDT, mediodorsal nucleus of thalamus; CM, centromedian nucleus of thalamus; CeA, central nucleus of amygdala; BLA, basolateral nucleus of amygdala; DMH, dorsomedial hypothalamus; VMH, ventromedial hypothalamus; AC, auditory cortex; EC, entorhinal cortex; vCA1, ventral cornu ammonis 1; vCA3, ventral cornu ammonis 3; vDG, ventral dentate gyrus; SN, substantia nigra; VTA, ventral tegmental area; PAG, periaqueductal area; DRN, dorsal raphe nucleus; PBS, phosphate buffered saline; and LPS, lipopolysaccharide.

https://doi.org/10.2147/JIR.S362006

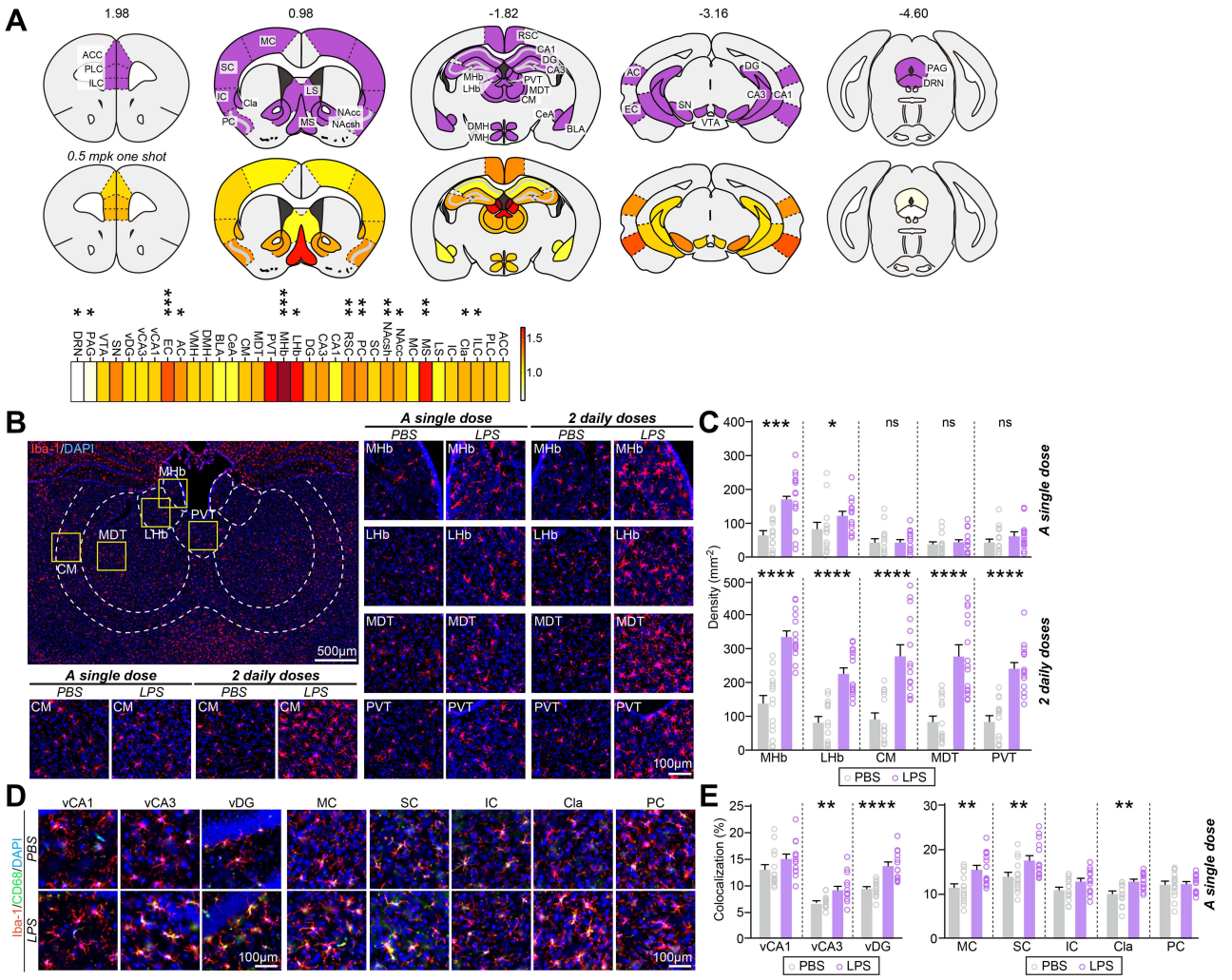

Figure 1 Mild, LPS-induced inflammation produces a spatially patterned microglial activation throughout the adult mouse brain. (**A**) Heat maps of fold changes in microglia number in each anatomical region induced by single i.p. LPS injection. Top: Purple represents brain regions examined; bottom: color scale indicates fold changes in microglia number ranging from 0 to 1.64; fold change in MHb is not included (2.61) (*p < 0.05, **p < 0.01, ***p < 0.001). (**B**) Representative images of MHb, LHb, CM, MDT or PVT brain regions and immunostaining for the microglial marker Iba-1 in mice injected with saline or i.p.-administered a single or 2 daily doses of LPS. (**C**) Quantification of the density of Iba-1$^+$ cells. Data are means ± SEMs (n = 14~15 sections from 5 mice; *p < 0.05, ***p < 0.001, ****p < 0.0001; Mann–Whitney U-test). (**D**) Representative images of vCA1, vCA3, vDG, MC, SC, IC, Cla or PC brain regions and immunostaining for the microglial marker Iba-1 and CD68 in mice injected with saline or i.p.-administered a single dose of LPS. Scale bar: 25 μm (applies to all images) (**E**) Quantification of the colocalization percentage of Iba-1$^+$/CD68$^+$ cells. Data are means ± SEMs (n = 14~15 sections from 5 mice; **p < 0.01, ****p < 0.0001; Mann–Whitney U-test).

Abbreviations: ACC, anterior cingulate cortex; AC, auditory cortex; BLA, basolateral nucleus of amygdala; CA1, cornu ammonis 1; CA3, cornu ammonis 3; CeA, central nucleus of amygdala; Cla, claustrum; CM, central nucleus of thalamus; DG, dentate gyrus; DMH, dorsomedial hypothalamus; DRN, dorsal raphe nucleus; EC, entorhinal cortex; IC, insula cortex; ILC, infralimbic cortex; LHb, lateral habenula; LS, lateral septum; MDT, mediodorsal nucleus of thalamus; MHb, medial habenula; MC, motor cortex; MS, medial septum; NAcc, nucleus accumbens core; NAcsh, nucleus accumbens shell; PAG, periaqueductal area; PC, piriform cortex; PLC, prelimbic cortex; PVT, paraventricular nucleus of thalamus; RSC, retrosplenial cortex; SC, somatosensory cortex; SN, substantia nigra; vCA1, ventral CA1; vCA3, ventral CA3; vDG, ventral DG; VMH, ventromedial hypothalamus; and VTA, ventral tegmental area.

these regions, the MHb displayed the largest fold change (~2.6-folds) in the number of microglia in mice injected with a single dose of LPS compared with control saline-injected mice (Table 1, Figure 1C).

To confirm whether the enhanced density of microglia induced by LPS administration represents a population of activated microglia, we performed an immunohistochemical analysis of the expression levels of CD68, a lysosomal protein that is frequently used as a marker for active phagocytic microglia.[17] Strikingly, CD68 expression was significantly increased in Cla regions, but not in MHb, LHb, NAc, EC or AC regions, following a single i.p. LPS injection, despite increases in microglia numbers (Figure 1D and E and Figure S3). Interestingly, CD68 expression was markedly increased in CA3 and DG of ventral hippocampal regions (vCA3, vDG), basolateral amygdala (BLA), and dorsomedial hypothalamus (DMH), where microglia numbers were unchanged by a single i.p. LPS injection (Figure 1D and E and Figure S3). These data suggest that microglia in

different brain regions are differentially activated by mild, LPS-induced inflammation relative to the increase in microglia numbers or increased CD68 expression.

Under systemic inflammatory condition, circulating monocytes from the bloodstream can infiltrate to the CNS.[18] Thus, we further investigated whether increases in the number of microglia in different brain regions of LPS-treated mice were attributable to infiltration of circulating monocytes into the brain. To this end, we examined the expression of chemokine (C-C motif) receptor 2 (CCR2), a marker of monocytes, using mice expressing red fluorescent protein (RFP) under the control of the *CCR2* promoter. Specifically, hemizygous *CCR2*-RFP ($CCR2^{RFP/+}$) mice were i.p.-injected with a single dose or 2 daily doses of saline or LPS, and then 24 h after the final LPS injection, brain tissues were examined histologically for invasion of circulating monocytes. These analyses revealed that, following a single i.p. LPS injection, the red fluorescence from RFP was barely detectable in some brain regions, such as the MHb, LHb, EC, nucleus accumbens core (NAcc) and nucleus accumbens shell (NAcsh), in which microglia numbers were increased (Figure 2). In contrast, in mice injected with two daily doses of LPS, red fluorescence-positive cells were prominently detected in VTA regions (Figure 2). These data imply that resident microglia rather than infiltrating monocytes likely contribute to the increased number of microglia in response to peripheral LPS administration.

Cytokines Released by Activated Microglia Exhibit Brain Region-Specific Differences

Given that low, tolerable doses of LPS render the brain transiently protect against subsequent neural injury,[18–20] we determined whether increases in microglia numbers or activation by a single low-dose injection of LPS lead to differentiation of microglia into an M1-type (pro-inflammatory) or M2-type (anti-inflammatory) phenotype. To this end, we performed quantitative RT-PCR to measure the mRNA levels of the anti-inflammatory cytokine genes, interleukin-4 (*IL-4*) and transforming growth factor-beta1 (*TGF-β1*), and pro-inflammatory cytokine genes, interleukin-1beta (*IL-1β*) and tumor necrosis factor-alpha (*TNFα*) in selected brain regions. For purposes of monitoring mRNA expression of inflammatory factors, we chose the Hb region, where microglia numbers were increased with no changes in CD68 expression; the hippocampal region, where CD68 expression was elevated with no change in microglial density; cortical regions, where microglia number and CD68 expression were increased; and the VTA region, where neither microglia number nor CD68 expression was changed. This analysis showed that mRNA levels of *IL-1β* and *TNFα* were significantly increased in hippocampal and Hb regions as well as cortical regions, with *IL-1β* exhibiting ~20

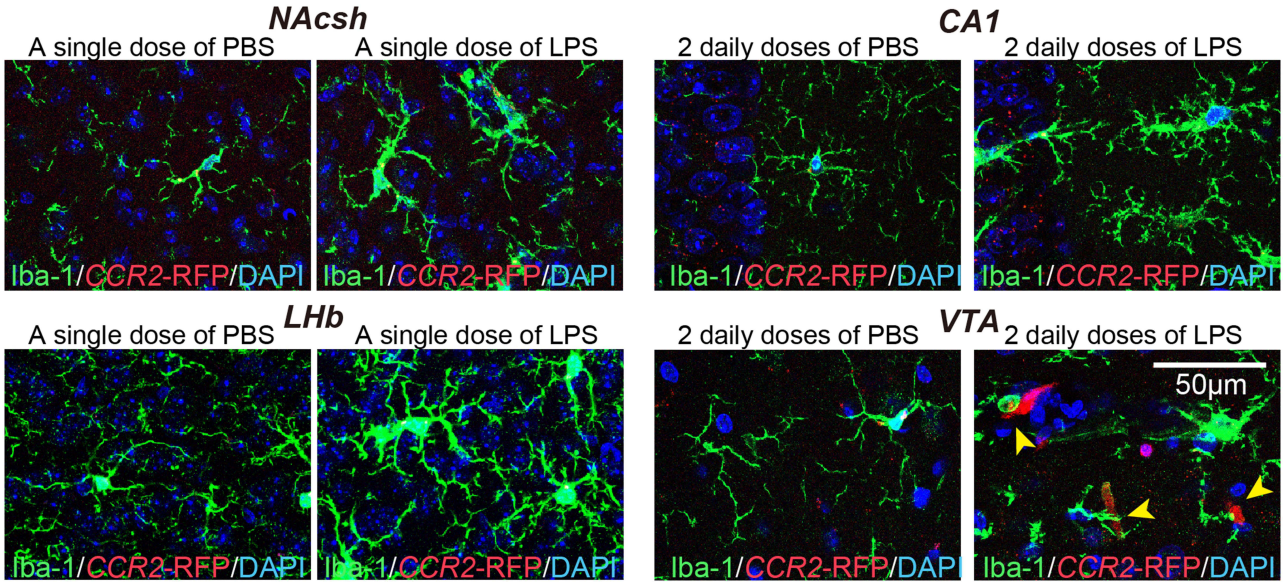

Figure 2 Mild, LPS-induced inflammation does not cause the infiltration of peripheral immune cells. Representative images showing the number of *CCR2*-RFP^+ cells and immunostaining for the microglial marker Iba-1 (green) in the indicated brain regions of *CCR2*-RFP mice injected with saline or i.p.-administered a single or 2 daily doses of LPS. Yellow arrow heads indicate *CCR2*-RFP^+ cells.

Abbreviations: CA1, cornu ammonis 1; LHb, lateral habenula; NAcsh, nucleus accumbens shell; and VTA, ventral tegmental area.

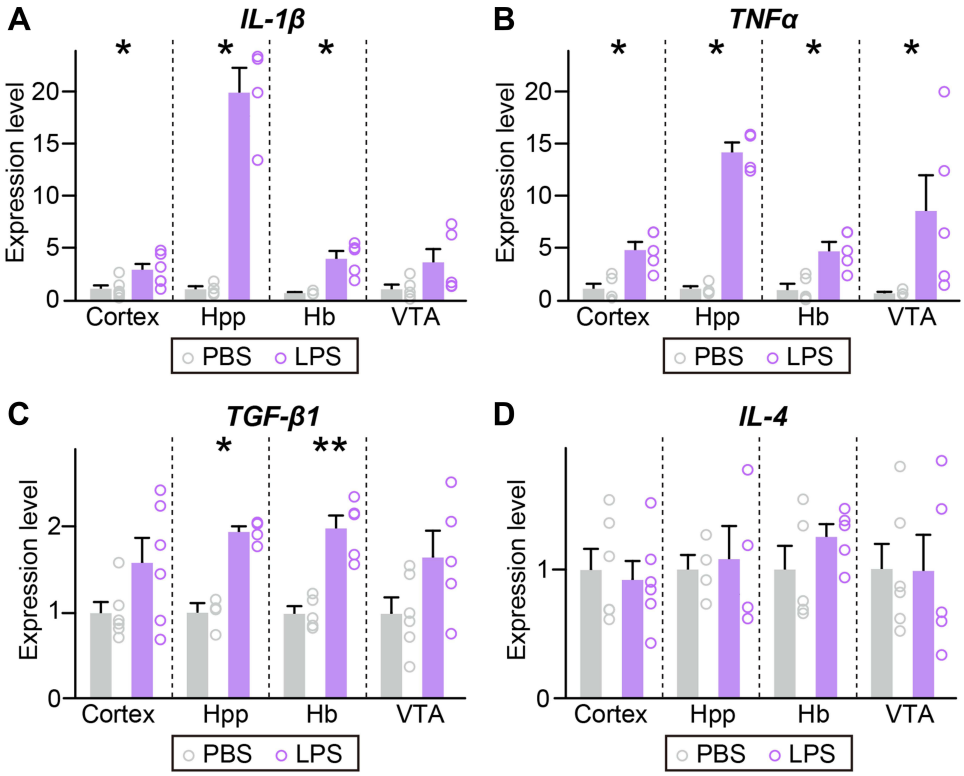

Figure 3 Mild, LPS-induced inflammation upregulates the pro-inflammatory cytokine levels. (**A–D**) qRT-PCR analysis of *IL-1β, TNFα, TGF-β1*, and *IL-4* in the indicated regions of brain collected from mice i.p.-injected with saline or a single dose of LPS. (n = 4~6 mice/group; *$p < 0.05$, **$p < 0.01$; Mann–Whitney *U*-test).
Abbreviations: Hb, habenula; Hpp, hippocampus; IL-1β, interleukin-1beta; IL-4, interleukin-4; TGF-β1, transforming growth factor-beta1; TNFα, tumor necrosis factor-alpha; and VTA, ventral tegmental area.

and ~5-fold increases in the hippocampus and Hb, respectively, and *TNFα* showing corresponding increases of ~15- and ~5-fold, whereas *TNFα* mRNA levels were moderately increased in the VTA region (Figure 3). *TGF-β1* mRNA levels were increased by ~2-fold in the hippocampus and Hb but were unchanged in the VTA (Figure 3), and *IL-4* mRNA levels were unchanged in all brain regions examined (Figure 3). These data suggest that microglia resident in brain regions, in which a single low-dose injection of LPS produced microglial changes, preferentially generated pro-inflammatory cytokines.

Discussion

In the current study, we sought to uncover which brain areas are vulnerable to neuroinflammation by applying a systemic inflammation-inducing protocol that causes mild neuroinflammation. We analyzed microglial alterations as a consequence of neuroinflammation in various brain regions and identified specific regions that exhibited higher vulnerability to neuroinflammation, detecting significant increases in the number of microglia in Hb, MS, NAc, Cla, ILC, PC, RSC, AC, and EC regions in response to a mild neuroinflammatory stimulus.

It has been reported that microglial proliferation is primarily observed in circumventricular organs (CVOs) lacking a typical blood-brain barrier (BBB) surrounding the brain ventricles and in the neighboring brain areas.[21,22] Thus, CVOs are considered to play key roles in mediating blood-brain communication, and can be reached directly by pathogens and cytokines through CVO capillaries, which further spread out to other brain regions.[21,22] The current study did not determine the extent to which increased numbers of microglia induced by mild inflammation are caused by an increased rate of microglial proliferation and/or increased recruitment of residual microglia. Future studies are warranted to address this important issue.

Microglia play important roles in synaptic pruning through the complement cascade during development and under disease conditions.[23–25] Microglial synaptic pruning contributes to determining the synaptic excitation/inhibition

balance and sculpting the properties of specific neural circuits.[26] In this context, neuroinflammation-induced changes in the key functions of microglia in Hb, MS, NAc, Cla, ILC, PC, RSC, AC, and EC regions may exert significant effects on synaptic/circuit functions and subsequent progression of specific and relevant neurological diseases. These brain regions have been reported to be associated with various neurological diseases.[13–16] Future studies should determine whether the microglial activation induced by mild neuroinflammation affects the phagocytic activities involved in synapse pruning or contributes to progression of relevant neuropsychiatric or neurodegenerative diseases in specific brain regions.

While neuroinflammation is induced by acute CNS injuries such as traumatic brain injury, spinal cord injury and stroke, microglia release pro-inflammatory cytokines and reactive oxygen species[27] that may be detrimental to recovery. In addition, peripheral immune cells are recruited and infiltrated into CNS tissue,[28] although whether this has a beneficial or detrimental impact on recovery is a matter of controversy. Unlike acute and strong neuroinflammation, mild neuroinflammatory conditions did not cause infiltration of peripheral immune cells, but activated resident microglia did release pro-inflammatory cytokines such as IL-1β or TNFα in neuroinflammation-vulnerable brain regions. Although more studies are required, considering that microgliosis and neuroinflammation are accompanied by poor clearance of β-amyloid by microglia in the brains of late stage AD patients, it is likely that the ability of microglia to sculpt synaptic connections through phagocytosis may be diminished under neuroinflammatory condition.[29]

Microglia are not uniformly distributed throughout the CNS; instead, they exhibit differences in characteristics among brain regions ranging from cell number and morphology to molecular signature. Thus, microglia may differentially function in a brain region-specific manner.[30] It is tempting to speculate that such spatial heterogeneity contributes to the varying sensitivities of individual microglia in different brain regions to neuroinflammatory signals, and hence underlies their functional relevance for CNS disease development. In particular, region-specific expression of microglial gene signatures relevant to inflammation might affect the properties and sensitivities of microglia. For example, TREM2 (triggering receptor expressed on myeloid cells 2) was found to be variably expressed; relatively high in the frontal cortex, NAc and hippocampus, but low in the thalamus, hypothalamus and SN.[31] CX3CR1 (C-X3-C motif chemokine receptor 1) expression was also shown to be enriched in cortical regions, basal ganglia and the hypothalamus compared with noncortical regions.[32] These molecular diversities might account for regional vulnerabilities to mild inflammation.

Our study has several limitations. First, we employed only male mice in the current study to minimize variability resulting from the effect of female hormones. Given the well-known sexual dimorphism among individuals with neuropsychiatric disorders, it would be worthwhile investigating whether the altered microglial density and/or activity observed in males is similarly recapitulated in their female counterparts. Second, we did not perform a detailed analysis of alterations in microglial morphology in response to mild neuroinflammation. Historically, microglia phenotypes have been classified into three categories based on their morphological features: ramified cells, designated “resting” microglia; bushy cells, considered intermediate states; and amoeboid cells, defined as activated microglia.[17,33] Given that microglia morphological features and functions are intimately correlated, such a further analysis of microglial morphology should be applied to our mouse model. Third, a variety of factors (eg, temporal sequences of neuroinflammation, molecular identities of microglia, stimulus dose, type of stimulus) could contribute to the various forms of microglial dynamics. Specific ligands mediate microglial activation through specific receptors to produce behavioral outcomes.[34] It is possible that an increased rate of microglial proliferation and/or increased infiltration of peripheral monocytes by neuroinflammation might depend on the type of stimulant. Therefore, it is important to assess whether observed changes in microglial density and/or activity are similarly recapitulated in a variety of conditions that induce neuroinflammation.

Overall, the current study identified specific neuroinflammation-sensitive brain regions that may be linked to neuroinflammation-associated brain malfunction or pathologies. Our observations provide important clues regarding future therapeutic targets against the pathobiology of neuroinflammation.

Conclusions

In this study, we identified specific regions that exhibited higher vulnerability to neuroinflammation, detecting significant increases in the number of microglia in the Hb, MS, NAc, Cla, ILC, PC, RSC, AC, and EC regions. Our findings

contribute to a better understanding of how systemic inflammation affects brain function and which brain regions are most and earliest affected, as well as a novel insight that changes in microglial function in specific brain regions caused by systemic inflammation may have significant effects on synaptic/circuit functions and the progression of specific, relevant neurological diseases.

Data Sharing Statement

The data sets analyzed during the current study are available from the corresponding author on reasonable request.

Ethics Approval

All procedures and protocols were approved by the Institutional Animal Care and Use Committee of Daegu Gyeongbuk Institute of Science and Technology (DGIST). All experiments were conducted according to the guidelines and protocols for rodent experimentation approved by the Institutional Animal Care and Use Committee of DGIST.

Consent for Publication

Not applicable.

Acknowledgments

We thank Jinha Kim (DGIST) for technical assistance.

Author Contributions

All authors made a significant contribution to the work reported, whether that is in the conception, study design, execution, acquisition of data, analysis and interpretation, or in all these areas; took part in drafting, revising or critically reviewing the article; gave final approval of the version to be published; have agreed on the journal to which the article has been submitted; and agree to be accountable for all aspects of the work.

Funding

This study was supported by grants from the National Research Foundation of Korea (NRF) funded by the Ministry of Science and Future Planning (2019R1A2C1086048 to J.W.U. and 2020R1A4A1019009 to E.C., Y.M.H., J.W.Y., and J.W.U.), the DGIST R&D Program of the Ministry of Science and ICT (22-CoE-BT-01, 22-HRHR-01 to J.W.U.).

Disclosure

The authors declare that they have no competing interest in this work.

References

1. Sochocka M, Diniz BS, Leszek J. Inflammatory response in the CNS: friend or foe? *Mol Neurobiol*. 2017;54(10):8071–8089. doi:10.1007/s12035-016-0297-1
2. DiSabato DJ, Quan N, Godbout JP. Neuroinflammation: the devil is in the details. *J Neurochem*. 2016;139(S2):136–153. doi:10.1111/jnc.13607
3. Manabe T, Heneka MT. Cerebral dysfunctions caused by sepsis during ageing. *Nat Rev Immunol*. 2021. doi:10.1038/s41577-021-00643-7
4. Tejera D, Mercan D, Sanchez-Caro JM, et al. Systemic inflammation impairs microglial Aβ clearance through NLRP3 inflammasome. *EMBO J*. 2019;38(17):e101064. doi:10.15252/embj.2018101064
5. Singer BH, Newstead MW, Zeng X, et al. Cecal ligation and puncture results in long-term central nervous system myeloid inflammation. *PLoS One*. 2016;11(2):e0149136. doi:10.1371/journal.pone.0149136
6. Olofsson PS, Rosas-Ballina M, Levine YA, Tracey KJ. Rethinking inflammation: neural circuits in the regulation of immunity. *Immunol Rev*. 2012;248(1):188–204. doi:10.1111/j.1600-065X.2012.01138.x
7. Tracey KJ. The inflammatory reflex. *Nature*. 2002;420(6917):853–859. doi:10.1038/nature01321
8. Cao P, Chen C, Liu A, et al. Early-life inflammation promotes depressive symptoms in adolescence via microglial engulfment of dendritic spines. *Neuron*. 2021;109(16):2573–2589. doi:10.1016/j.neuron.2021.06.012
9. Pires JM, Foresti ML, Silva CS, et al. Lipopolysaccharide-induced systemic inflammation in the neonatal period increases microglial density and oxidative stress in the cerebellum of adult rats. *Front Cell Neurosci*. 2020;14:142. doi:10.3389/fncel.2020.00142
10. Wang KC, Fan LW, Kaizaki A, Pang Y, Cai Z, Tien LT. Neonatal lipopolysaccharide exposure induces long-lasting learning impairment, less anxiety-like response and hippocampal injury in adult rats. *Neuroscience*. 2013;234:146–157. doi:10.1016/j.neuroscience.2012.12.049

11. Fan L-W, Tien L-T, Zheng B, et al. Dopaminergic neuronal injury in the adult rat brain following neonatal exposure to lipopolysaccharide and the silent neurotoxicity. *Brain Behav Immun*. 2011;25(2):286–297. doi:10.1016/j.bbi.2010.09.020
12. Zheng Z-H, Tu J-L, Li X-H, et al. Neuroinflammation induces anxiety- and depressive-like behavior by modulating neuronal plasticity in the basolateral amygdala. *Brain Behav Immun*. 2021;91:505–518. doi:10.1016/j.bbi.2020.11.007
13. Aizawa H, Cui W, Tanaka K, Okamoto H. Hyperactivation of the habenula as a link between depression and sleep disturbance. *Front Hum Neurosci*. 2013;7. doi:10.3389/fnhum.2013.00826
14. Fenster RJ, Lebois LAM, Ressler KJ, Suh J. Brain circuit dysfunction in post-traumatic stress disorder: from mouse to man. *Nat Rev Neurosci*. 2018;19(9):535–551. doi:10.1038/s41583-018-0039-7
15. Hu H, Cui Y, Yang Y. Circuits and functions of the lateral habenula in health and in disease. *Nat Rev Neurosci*. 2020;21(5):277–295. doi:10.1038/s41583-020-0292-4
16. Russo SJ, Nestler EJ. The brain reward circuitry in mood disorders. *Nat Rev Neurosci*. 2013;14(9):609–625. doi:10.1038/nrn3381
17. Park D, Kim S, Kim H, Shin J, Jung H, Um JW. Seizure progression triggered by IQSEC3 loss is mitigated by reducing activated microglia in mice. *Glia*. 2020;68(12):2661–2673. doi:10.1002/glia.23876
18. Chen Z, Jalabi W, Shpargel KB, et al. Lipopolysaccharide-induced microglial activation and neuroprotection against experimental brain injury is independent of hematogenous TLR4. *J Neurosci*. 2012;32(34):11706–11715. doi:10.1523/JNEUROSCI.0730-12.2012
19. Tasaki K, Ruetzler CA, Ohtsuki T, Martin D, Nawashiro H, Hallenbeck JM. Lipopolysaccharide pre-treatment induces resistance against subsequent focal cerebral ischemic damage in spontaneously hypertensive rats. *Brain Res*. 1997;748(1):267–270. doi:10.1016/S0006-8993(96)01383-2
20. Shpargel KB, Jalabi W, Jin Y, Dadabayev A, Penn MS, Trapp BD. Preconditioning paradigms and pathways in the brain. *Cleve Clin J Med*. 2008;75(3 suppl 2):S77–S82. doi:10.3949/ccjm.75.Suppl_2.S77
21. Furube E, Kawai S, Inagaki H, Takagi S, Miyata S. Brain region-dependent heterogeneity and dose-dependent difference in transient microglia population increase during lipopolysaccharide-induced inflammation. *Sci Rep*. 2018;8(1):2203.
22. Torii K, Takagi S, Yoshimura R, Miyata S. Microglial proliferation attenuates sickness responses in adult mice during endotoxin-induced inflammation. *J Neuroimmunol*. 2022;365:577832. doi:10.1016/j.jneuroim.2022.577832
23. Stevens B, Allen NJ, Vazquez LE, et al. The classical complement cascade mediates CNS synapse elimination. *Cell*. 2007;131(6):1164–1178. doi:10.1016/j.cell.2007.10.036
24. Hong S, Beja-Glasser VF, Nfonoyim BM, et al. Complement and microglia mediate early synapse loss in Alzheimer mouse models. *Science*. 2016;352(6286):712–716. doi:10.1126/science.aad8373
25. Vasek MJ, Garber C, Dorsey D, et al. A complement–microglial axis drives synapse loss during virus-induced memory impairment. *Nature*. 2016;534(7608):538–543. doi:10.1038/nature18283
26. Um JW. Roles of glial cells in sculpting inhibitory synapses and neural circuits. *Front Mol Neurosci*. 2017;10. doi:10.3389/fnmol.2017.00381
27. David S, Kroner A. Repertoire of microglial and macrophage responses after spinal cord injury. *Nat Rev Neurosci*. 2011;12(7):388–399. doi:10.1038/nrn3053
28. Gelderblom M, Leypoldt F, Steinbach K, et al. Temporal and spatial dynamics of cerebral immune cell accumulation in stroke. *Stroke*. 2009;40(5):1849–1857. doi:10.1161/STROKEAHA.108.534503
29. Lai AY, McLaurin J. Clearance of amyloid-β peptides by microglia and macrophages: the issue of what, when and where. *Future Neurol*. 2012;7(2):165–176. doi:10.2217/fnl.12.6
30. Tan Y-L, Yuan Y, Tian L. Microglial regional heterogeneity and its role in the brain. *Mol Psychiatry*. 2020;25(2):351–367. doi:10.1038/s41380-019-0609-8
31. Schmid CD, Sautkulis LN, Danielson PE, et al. Heterogeneous expression of the triggering receptor expressed on myeloid cells-2 on adult murine microglia. *J Neurochem*. 2002;83(6):1309–1320. doi:10.1046/j.1471-4159.2002.01243.x
32. Tarozzo G, Bortolazzi S, Crochemore C, et al. Fractalkine protein localization and gene expression in mouse brain. *J Neurosci Res*. 2003;73(1):81–88. doi:10.1002/jnr.10645
33. Li D, Lang W, Zhou C, et al. Upregulation of microglial ZEB1 ameliorates brain damage after acute ischemic stroke. *Cell Rep*. 2018;22(13):3574–3586. doi:10.1016/j.celrep.2018.03.011
34. Murayama S, Kurganov E, Miyata S. Activation of microglia and macrophages in the circumventricular organs of the mouse brain during TLR2-induced fever and sickness responses. *J Neuroimmunol*. 2019;334:576973. doi:10.1016/j.jneuroim.2019.576973